
	<p style="text-align: center;">Bulletin of Scientific Contribution GEOLOGY</p> <p style="text-align: center;">Fakultas Teknik Geologi UNIVERSITAS PADJADJARAN</p> <p style="text-align: center;">homepage: http://jurnal.unpad.ac.id/bsc p-ISSN: 1693-4873; e-ISSN: 2541-514X</p>	 <p style="text-align: center;">Volume 23, No.2 Agustus 2025</p>
---	---	---

DELINIATION OF SHALLOW GAS ZONE POTENTIAL USING SUBSURFACE DATA APPROACH IN 'X' FIELD KUTAI BASIN

Yuyun Yuniardi, Febriwan Mohammad, M. Kurniawan Alfadli, Nanda Natasia, Andi Agus Nur

Faculty of Geology, Padjadjaran University
Jalan Ir. Soekarno KM. 21 Jatinangor 45393
Email : yuyun.yuniardi@unpad.ac.id

ABSTRACT

The presence of shallow gas (Shallow Gas) in exploration wells poses significant operational risks, including kicks or blowouts during exploration activities. To mitigate these risks, it is essential to delineate subsurface data and identify areas potentially containing shallow gas. Subsurface interpretation was conducted using various datasets, including electrolysis cutting analysis, well log data (GR, RT, NEU, RHOB) from 39 wells, and gas data obtained from chromatograph-based mud logs. Well correlation was performed to identify anomalies, gas presence, and facies characteristics.

The stratigraphy of Platform M is dominated by a thick Neogene succession composed of fluvial-deltaic, coastal, and shallow marine deposits. These successions reflect the evolution of the Mahakam Delta, influenced by high sediment supply, relative sea-level fluctuations, and structural subsidence. Detailed analysis reveals a stratigraphic architecture consisting of stacked deltaic sequences, marked by progradational, aggradational, and retrogradational patterns. These sequences are bounded by regional unconformities and maximum flooding surfaces, indicating cyclic sedimentation controlled by tectonics and eustasy. The primary stratigraphic marker surfaces indicative of shallow intervals in Field X are, from deeper to shallower, MF2, Fs-s1, s2-Fs, Fs-s3, Fs-s4, Fs-s5, and Fs-s6, with the shallow gas accumulation predominantly observed within the intervals associated with Fs-s2 and Fs-s3, at depths ranging from approximately 950 to 1300 meters below sea level (MSS). These intervals demonstrate isolated gas accumulations, primarily comprising methane (C1), with minor traces of C2, C3, C4, and C5 gases detected in the shallow zone above the marker MF2.

Gas analysis indicates a surge in total gas content within the 950-1300 MSS interval, correlating with anomalies identified from the Master Log data. This surge is attributed to limestone and coal layers, as corroborated by gas bearing reservoir mapping.

Based on the analyzed data, it can be concluded that shallow gas accumulations are localized within the 950-1300 MSS interval, specifically between the Fs-s2 and Fs-s3 markers. For subsequent drilling activities on Platform M, it is recommended to monitor and consider this depth zone to mitigate related risks effectively.

Keywords: *Electrofacies Analysis, Deliniation, Gas Analysis, , Marker Interval, Shallow Gas, Well Correlation.*

INTRODUCTION

The Kutai Basin, located in East Kalimantan, Indonesia, is one of the most significant hydrocarbon provinces in Southeast Asia, renowned for its extensive oil and gas reserves. Recognized as the widest and deepest sedimentary basin in Central Indonesia, it spans an area of approximately 60,000 km² with sediment thicknesses reaching up to 15,000 meters (Banerjee & Salim, 2020; Mora et al., 2000). The basin's

complex geological history—shaped by tectonic activity, prolonged sedimentation, and thermal maturation—has led to the development of multiple hydrocarbon accumulations across various stratigraphic levels (Nainggolan et al., 2021).

Primarily derived from Tertiary deltaic systems and fluvial depositional environments, the Kutai Basin plays a vital role in the petroleum system of East Kalimantan Province, hosting numerous oil

and gas fields, many of which have been actively explored and developed (Bachtar, 2018; Colke et al., 1999). Given this long-standing history of hydrocarbon exploration and production, particularly in the Mahakam Delta, a comprehensive understanding of the spatial distribution and characteristics of shallow gas accumulations within the basin is essential. Such knowledge is critical for optimizing drilling operations, minimizing operational risks, and improving resource recovery (Koning et al., 2021).

This study specifically investigates the southern part of the Mahakam Delta—an area within the Kutai Basin—where the shallow

formations are composed of interbedded sandstones and claystones, along with intercalations of coal and limestone. Some of these sandstone layers contain shallow gas, which can increase formation pressure and pose a risk of blowouts during drilling. Therefore, detailed assessments of shallow gas zones are necessary to support safe and efficient drilling operations. The variability in hydrocarbon field sizes and column heights across the region further illustrates the complexity of the petroleum system, reflecting the interplay of stratigraphic, structural, and depositional controls (Napitupulu et al., 2021).

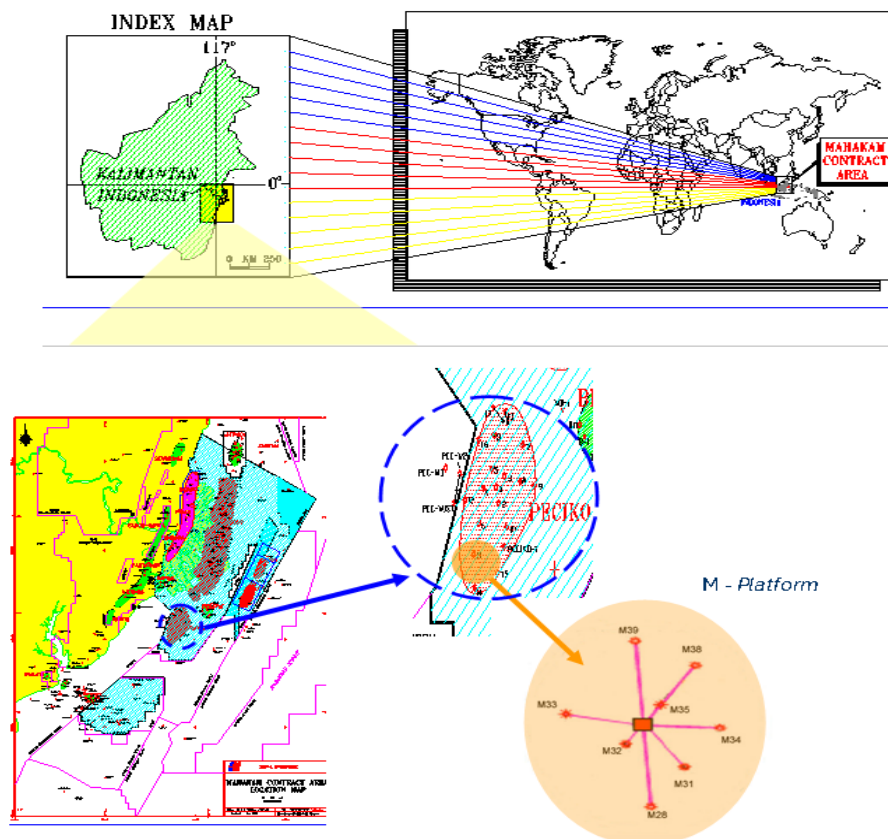


Figure 1 illustrates the precise location of the research area, which is primarily focused on exploration activities within the 'X' Field. This field is situated in the Kutai Basin, an extensive sedimentary basin located in East Kalimantan, Indonesia. The map provides a detailed geographic context, highlighting the spatial relationship of the 'X' Field relative to surrounding geological features. Understanding this location is crucial for interpreting the geological characteristics and exploration strategies employed within the basin.

The "X" field within the Kutai Basin offers a valuable opportunity to examine the occurrence and characteristics of shallow gas accumulations within a complex geological framework. Accurate delineation of these shallow gas zones is critical for ensuring safe and efficient drilling operations, as well as for optimizing subsurface resource exploitation. Shallow gas is a prevalent feature in many sedimentary basins and presents notable

challenges during drilling, including potential pressure increases, kicks, and blowouts. In this study, the analysis is focused specifically on Platform M, located within the southern part of the Mahakam Delta, which is part of the X field. This area has been observed to contain shallow gas zones based on historical drilling data and gas anomalies encountered during well operations. Therefore, Platform M serves as a representative area for understanding

shallow gas occurrences within the Kutai Basin.

The objective of this study is to analyze the correlation between various log data—including gamma ray (GR), resistivity (RT), neutron porosity (NPHI), density (RHOB), sonic, and chromatograph gas data—collected from eight wells drilled on Platform M. This analysis directly supports the research theme by aiming to identify reliable geological and petrophysical markers that indicate shallow gas presence and distribution. Through advanced analytical techniques, the study further seeks to characterize electrofacies within the research area, providing insights into fluid content, gas anomalies, and potential zones of instability, such as blowout-prone intervals.

By linking subsurface gas signatures to log responses and lithological variations, this research contributes directly to shallow gas detection, risk assessment, and hazard mitigation—core themes within the context of safe hydrocarbon exploration and development in the Mahakam Delta. The expected outcomes of this research include establishing a reference framework for identifying shallow gas zones, thereby enhancing safety measures and reducing the risk of blowouts during drilling operations.

METHODOLOGY

This study encompasses the shallow zone (± 1500 mSS) or to the marker regional marker MF2 (seismic based). The first stage began with a literature study and collect data that will be used, involving for electrofacies interpretation and gas chromatograph interpretation until ± 1500 mSS (shallow zone, until MF2 of marker limit). This study used the wireline logs data: gamma ray (GR), resistivity (RT), neutron (NPHI), density (RHOB) of 39 developed wells. Thus, it results the stratigraphic cross-section which is positioned based on regional marker stratigraphic of MF2 surface (Gastaldo, 1992). The second stage is to determine the electrofacies in the study area. The well-log data sets in the LAS format were imported into Interactive Petrophysics software for analysis. Cluster analysis to determine the type of electrofacies are used to identify the zones of lithology, porosity and permeability. Petrophysical parameters such as shale volume, porosity and water saturation were calculated from well logs. Gas data is used to see the hydrocarbon content, type of gas and the interval of gas surge in the study area. The final stage is to make subsurface interpretation based on existing data, and then to conduct correlation between the data to determine the distribution of the shallow gas.

In this study, the analysis conducted based on electrofacies data and wells correlation data, which is referred to GR log data to find the best lithological interpretation of clastic sedimentary rock. Analog models used modern models of Mahakam Delta which is classified as fluvial-tidal dominated (Allen et al., 1998) (Chen, 2018; Hasan et al., 2023; Kompanik et al., 1993). For well correlation, the correlation method used Maximum Flooding Surface (MFS), then the stratigraphic correlation was done throughout the interval study (Drake et al., 2013; Nur et al., 2020). Of each interval sequence is used for the making of Net To Gross map. This comparison was made to describe the pattern of sandstone spread in each sequence and explains the relationship between sequences (Asquith, 1982). (Al-Aziz et al., 2009; Pendkar et al., 2014) To study the spread pattern of gas in the reservoir of platform M, it is performed the correlations detail at several intervals to have predict the largest gas content. The interval limited by surface flooding, then each of it is made as the determination and correlation between reservoirs with GR log parameters (cut off 40%). Correlation detail used to explain the distribution of the net sand reservoir based maps created on each unit reservoir.

Digital image processing techniques are also relevant in this domain, specifically for analyzing geophysical survey data (Amalia, 2019).

RESULT AND DISCUSSION

Lithofacies

Lithofacies cutting analysis is done by using the data that is used as substitute for core data. Cutting data is taken from wells M34 which is considered to represent 8 wells from Platform M. A total of 12 layer packages can be identified in which the deposition of the package to seven to ten shows differences in the characteristics of the sediment that has not compacted. In general depositional pattern consists of thin interlayer between coarse sand and clay that appear as inserts. At this deposition package thinner sand deposition or by deposition of clay and there are fossil traces such as shells and wood fragments, which shows the influence of fluvial. Based on the characteristics of the sludge, it can be concluded that the facies is dominated as the transition of muddy sands and shallow sub-tidal to intertidal mudflats in front delta environment. From the foregoing, it is concluded that the pattern of deposition generally to a depth of 1500 mSS showed the interlayer between sandstone and mudstone with traces of limestone and lignite in the form of a thin insertion deposited on Shallow zone.

The integration of sequence stratigraphy and seismic attribute analysis offers a robust methodology for characterizing subsurface geological features and identifying potential hydrocarbon reservoirs ([Syed et al., 2008](#)). The absence of comprehensive data on sedimentation hinders the understanding of sand body development and physical property regulations ([Yang et al., 2023](#)).

Electrofacies and Fluid Content

In facies interpretations to determine the location that contains gas or fluid, the thing to do is to analyze the log response especially those that have the characteristics of log response with low GR, large resistivity log, and separation is found between neutron logs and density log found. Software-driven analysis of electrofacies distribution across wells delineates variations in their respective sedimentary and fluid properties. Electrofacies analysis reveals distinct characteristics of reservoir zones, aiding in the identification of potential hydrocarbon-bearing intervals ([Graña et al., 2012](#)). Electrofacies classification using well-log data serves as an alternative approach, especially when core data is limited ([Hasan et al., 2023](#)).

These characteristics show the gas content (not found any oil content in this field). On the layers of sandstones are interpreted as containing gas. A critical component of reservoir characterization involves spatially mapping facies variations, where the generation of one-dimensional (1D) facies models—informed by core samples, well logs and drilling reports obtained at discrete well locations—forms an essential preliminary step toward constructing comprehensive three-

dimensional facies models ([Keynejad et al., 2020](#)).

Result analysis of log response above show that at depth of ± 1050 – 1060 mSS, ± 1062 – 1077 mSS, and ± 1097 – 1108 mSS have sandstone lithology. This layer has the characteristics of log fining upwards (fining upward) and blocky and generally have a lower limit / base sharp (sharp base). Based on the characteristics of the log and supported by a thick layer is thick enough, it can be interpreted that the facies is channel. Meanwhile, at a depth of ± 1133 – 1136 mSS, ± 1142 – 1155 mSS, and ± 1162 – 1165 mSS based on log interpretation is known that the lithology is sandstones. This layer has the characteristics of log coarsening upwards with an average thickness of thin layers. Based on the characteristics of the log, it can be interpreted that the lithology is mouth bar.

Stratigraphic Section of 39 Wells

The stratigraphic positioning surface is determined by the Maximum Flooding Surface (MFS) in one cycle delta (transgressive and regressive). It is the background of the determination of the marker in this study. Naming marker after MF2 (Maximum Flooding which has limestone lithology) used as Fs-sx (flooding surface-shallow interval). For the determination of the marker in this study carried out only until the marker Fs-s6. Overall, it can be concluded that the marker Fs-s3, sediment deposition is the most regressive or show the most proximal sediment characteristics (Holm, 1998). Sediments forming the reservoir is good which is indicated by the present of seal in the form of claystone, so that the gas accumulates and does not spread. e sea

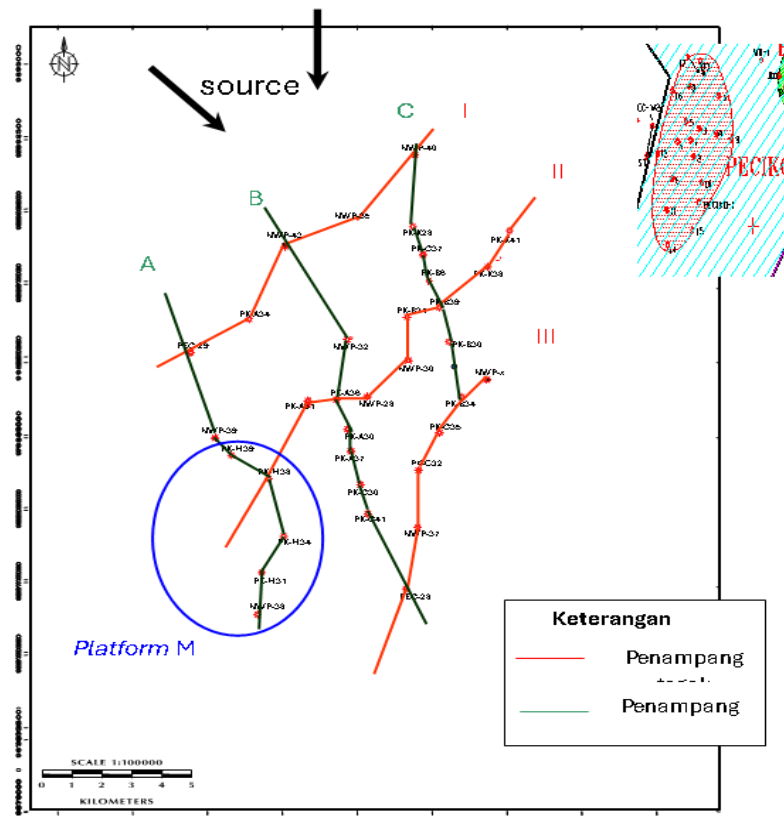


Figure 2. Well Log Section of Well M39 Showing Potential Shallow Gas accumulation within the Fs-s2 to Fs-s3 Marker Interval

Figure 2 presents a well log section for Well M39, specifically highlighting the interval known to contain shallow gas accumulations on Platform M. The logs likely displayed include Gamma Ray, Resistivity, and Total Gas, allowing for the identification of lithology, porosity, and gas anomalies. Of particular importance is the depth range between 1,000–1,300 mSS, corresponding to the stratigraphic interval bounded by the Fs and Fs-s3-s2 markers [Fs-s2][Fs-s3]. This figure likely illustrates how gas anomalies, identified by increased Total Gas readings, correlate with specific lithological units (possibly limestone and coal as seen in well M34), and how these anomalies align with the key stratigraphic markers in the area [Fs-s2][Fs-s3]. The figure helps to visualize the relationship between gas accumulation, lithology, and stratigraphic framework in Well M39.

The next thing is the comparison with the data observed cutting of the drilling results (master log) to see the similarities and differences in the interpretation of results. Similarities among others such as boundary precipitation package 1, equal to the limit of the maximum transgression on the marker Fs-s1 and limits of the package precipitation of 7.9, and 11 equal to the limit of the maximum transgression of marker-s4 Fs, Fs-s5, and Fs-s6. This proves that there is

equality of the data cutting and log data because both are equally lithology reflects the state of a region and both can be used to determine the marker. Next is the correlation unites the vertical log of each well within a stratigraphic cross-section of 39 horizontal wells and correlate markers predetermined. In the manufacture of stratigraphic cross-section (Based on the model of modern Mahakam Delta) to use a cross-correlation is directed perpendicular to the direction of progradation, because on this cross section is consistent with the sandstones sediment (getting to South direction and East, will be found more distal sediment dominant than the northern and western regions of the study area) than mudstone along the track making it easier to analyze the coating, thickness, lens, and so on.

Gas Distribution as Platform M

Based on the cross-section of the Platform M (relative trending North-South) made can be seen that the existence of shallow gas is at maximum marker interval Fs-s2 (in wells PK-M31, M33-PK, PK and PK-M38-M39) and Fs -s3 (on the well-M28 PK, PK and PK-M34-M39). Gas is generally accumulated in sandstones of the deposition channel and mouth bar with varying thickness. Of the cross, look for the spread of the gas and indicate if the gas is trapped. From the

schematic map (without scale) 3-D has proved that the shallow gas trapped in reservoir. Sediment are generally isolated in the sense of touch (disconnected) with sand other body (in an equal reservoir laterally). This shows that the sealing on the research is effective so that the gas does not move and isolated.

Sand to Sand Correlation

The division is based on the cycles of the delta (transgressive and regressive) in smaller intervals. Division marker is done by using the same manner as the previous marker determination. The markers are Fs-S1.1 Fs, Fs-S1.2, S1.3-Fs, Fs-S2.1, Fs-s2.2, Fs-S2.3. From the log data can be seen that the

marker interval Fs-s3 sediment depositions are more regressive than the marker interval Fs-s2 (visible from the log on wells M34). At intervals of Fs-s2 marker after correlated, it turns out there are 7 reservoirs (Fs-S1.3-c, Fs-S1.3-c, Fs-b-S1.3, S1.3-a-Fs, Fs-s1. 2-b, S1.2-a-Fs, Fs-S1.1) containing gas, which are not all connected. While the marker interval Fs-s3, there are 6 reservoirs (Fs-s3, Fs-S2.3-b, Fs-S2.3-a, Fs-b-s2.2, s2.2-a-Fs, Fs-S2.1) containing gas. Thus marker interval Fs-s2 created map structure and its Net To Gross (Figure 4), as well as intervals of Fs-s3 (Figure 5). In the manufacture of structural map author uses the form of software tools to map the CPS 3 while its Gross Net To use the method of "free hand".

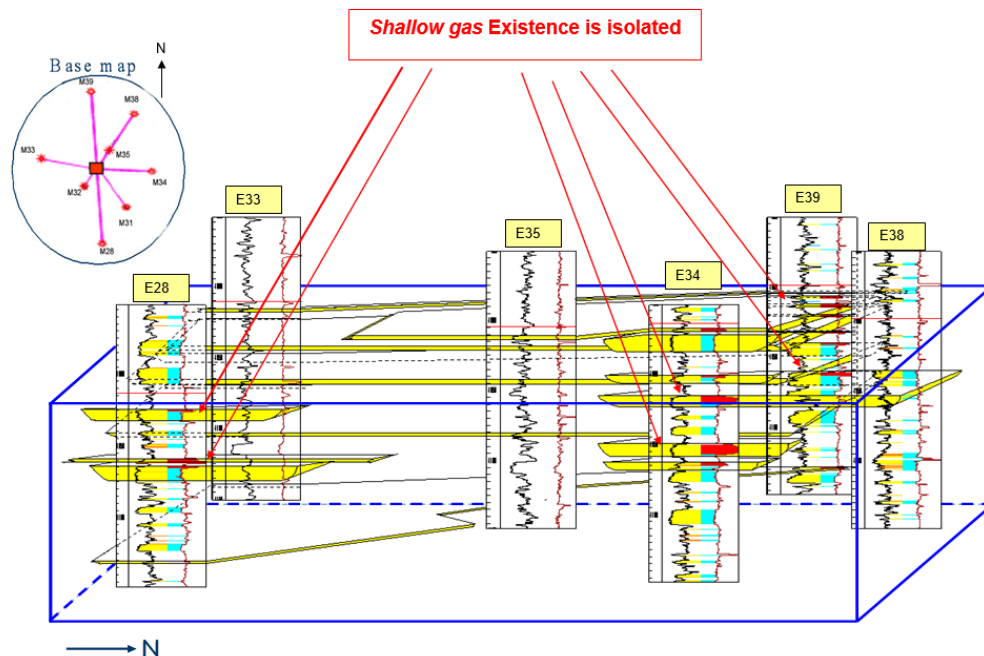


Figure 3 shows a schematic diagram of the Fs-S3 reservoir, highlighting locations with indications of shallow gas presence within each well.

The diagram is intended to provide a visual representation of the spatial distribution of shallow gas across the reservoir, with annotations indicating specific well locations and correlating gas presence. The Fs-S3 reservoir, as depicted in the schematic diagram, reveals a complex distribution of shallow gas accumulations across the platform (Abraham et al., 2020). The Fs-S3 reservoir exhibits a heterogeneous architecture wherein interconnected sand bodies serve as primary conduits for gas migration, thus dictating the spatial arrangement and concentration of shallow gas pockets observed throughout the formation.

Based on both these maps (Figures 4 and 5), of its isobath map shows that the platform marker M at intervals of Fs-Fs-s2 and s3 is located on a ridge (which may lead to the presence of shallow gas accumulation), especially in the marker interval Fs-s3 (Figure 5). This proves or supports a structural correlation data which describes an anticline (maximum on wells M34). The thickness of sandstones accumulated in wells M39, M34 and M28 (marked with a light green shading). After compared with the log cross section in Figure 3.4, it turns out at intervals of Fs-s3, concentrated on the shallow gas wells (M39, M34 and M28).

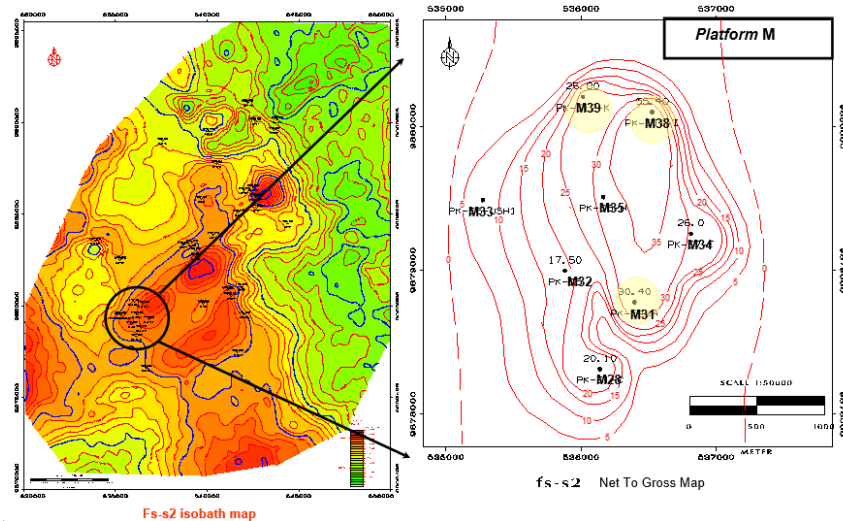


Figure 4. Isobath map and Net to Gross map for Fs-s2 marker interval, M Platform.

Figure 4 shows the isobath map and Net to Gross map for the Fs-s2 marker interval on Platform M, providing insights into the structural and sedimentological characteristics of the reservoir. The isobath map visualizes the depth contours of the Fs-s2 marker, enabling the identification of

structural features such as anticlines, synclines, and faults, while the Net to Gross map illustrates the proportion of reservoir-quality sandstone within the Fs-s2 interval, offering valuable information about reservoir heterogeneity and potential hydrocarbon accumulation zones.

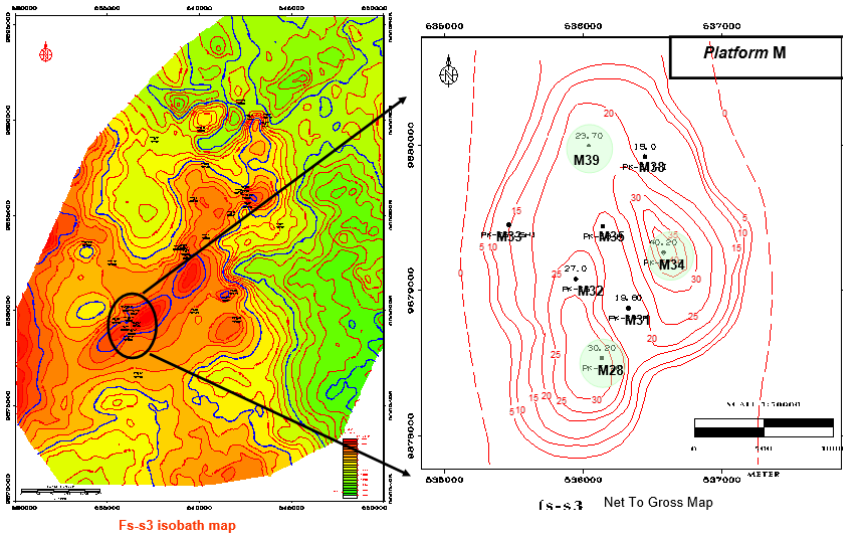


Figure 5. Isobath map and Net to Gross map for Fs-s3 marker interval, M Platform.

Figure 5 illustrates the isobath map and Net to Gross map for the Fs-s3 marker interval on Platform M, providing additional insights into the reservoir's structural and sedimentological attributes. The isobath map delineates the depth contours of the Fs-s3 marker, shedding light on structural features and their influence on reservoir architecture. The Net to Gross map highlights the distribution of reservoir-quality sandstone within the Fs-s3 interval, facilitating the identification of potential hydrocarbon accumulation zones and informing reservoir characterization efforts.

Figures 4 and 5 present a comparative analysis of the Fs-s2 and Fs-s3 marker

intervals on Platform M, utilizing isobath and net-to-gross maps to delineate structural and reservoir characteristics. By examining the isobath maps, one can discern the structural framework of each interval, identifying potential fault patterns and variations in horizon depths, which are critical for understanding the subsurface architecture. Comparing the net-to-gross maps reveals the distribution of reservoir-quality sands within each interval, highlighting areas of high sand concentration that are indicative of potential accumulation zones. Integrating both datasets allows for the identification of prospective locations where structural highs coincide with favorable reservoir properties,

thereby pinpointing potential shallow gas accumulation zones within the 950-1300 mSS interval [Fs-s2][Fs-s3]. According to the document, shallow gas tends to accumulate in sand bodies [Fs-s2] within this depth range. This integrated approach is essential for guiding drilling activities and risk mitigation on Platform M [Fs-s2][Fs-s3].

Gas Analysis

Combining master log and data LWD done to determiner gas anomaly on the master log readings and data LWD one of the wells the M34 wells. Gases like these that must be considered in the drilling process. Results of the comparison chart made show that if $C1 / TG$ (Total Gas) ≥ 0.9 , emerging gas is dominated by gas C1 (methane) and there are no other heavy gases (comparison of its gas log as in Figure 3.5 (Appendix) for M34 wells. If $C1 / TG \leq 0.9$ and compared with its gas logs, start there are other heavy gases although only minor traces and not too big. the data of its Master Log anomaly turns it originates from layers of limestone and coal (to be cautious on the limestone layer, due to high TG which means greater porosity, because if not careful can lead to loss (mud drilling lost into layers).

After that, it turns out there are some anomalies (high TG and $C1 / TG \leq 0.9$) (anomalies marked by blue circles or squares). Having drawn a line / area which is an area of anomaly, it turns out these anomalies are at a depth interval between 1.000–1.300 when compared with the MSS its log cross section, was included in the marker interval Fs and Fs-s3-s2 (where shallow gas accumulation).

Danger Zone on the Platform M Views of Seismic in Shallow Gas

In this study the seismic data used are seismic amplitude anomalies which uses the principle of the response of layers with high and low impedance. From seismic maps are made, it can be proven that in the interval 950-1300 or at intervals marker mSS Fs-s2-Fs-s3 indeed there is shallow gas accumulation.

In some wells at certain intervals clearly visible to the accumulation of gas, but at other intervals are not visible or only vaguely (small anomaly). its total gas shows that most of the gas accumulation show readings Total Gas > 5% (Background Gas was only 2-3% (master log), it indicates that there is a significant increase in gas which means it may cause hazards.

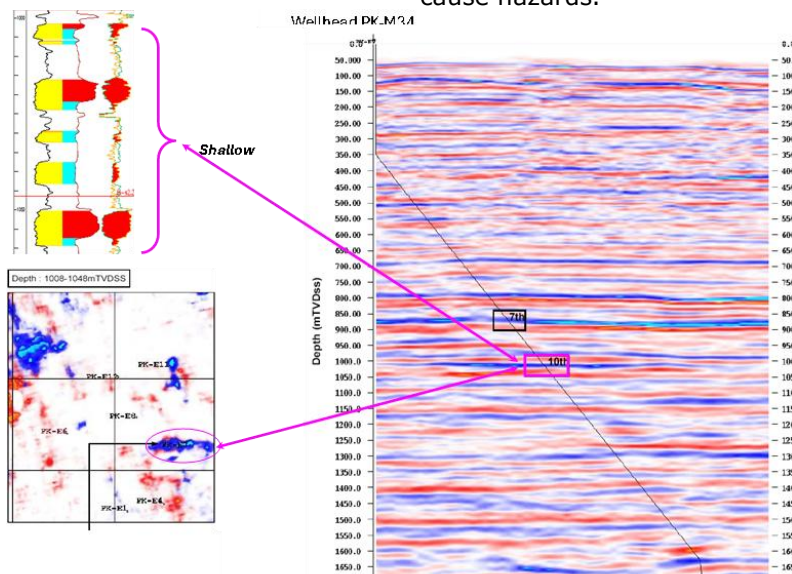


Figure 6. Shallow gas from seismic anomaly in well M34 in Platform M.

Figure 6 shows a seismic anomaly indicating shallow gas accumulation in well M34 on Platform M, providing valuable insights into the subsurface distribution of gas reservoirs. The seismic anomaly, characterized by distinct amplitude variations, suggests the presence of gas-filled zones within the geological strata. Analysis of the seismic data reveals the spatial extent and geometry of the shallow gas accumulation, aiding in risk assessment and mitigation strategies during

drilling operations. The well M34's seismic data shows a clear anomaly suggesting the presence of shallow gas. The total gas readings surpassing 5% indicate a substantial gas increase, posing potential hazards.

Gas Bearing Reservoir Mapping

The results of the interpretation of these maps indicates that the shallow gases (illustrated by the shaded portion in red) accumulates on a sand body and does not

spread or isolated existence (this is what causes the shallow gas this dangerous), and proves that the sealing on the platform M is effective. The shallow gas generally accumulates on the tops of the thickness of sediment sandstones, and spread following the contours of its depth (the result of the intersection of the sandstone thickness map (Net Sand) with its depth structure maps (isobath)). Based on these maps, then for the next drilling activity on Platform M, it is expected to be more careful when going into the depth interval between 950 - 1300 MSS, because in the interval has proved there is accumulation of gas in reservoir, and the presence in general isolated so be wary.

Potential Area of *shallow gas*

A significant shallow gas accumulation within the 950-1300 mSS interval, corresponding to the Fs-s3 to Fs-s2 marker intervals on Platform M. Seismic data confirms the presence of this gas, revealing amplitude

anomalies indicative of high and low impedance layers, with total gas readings frequently exceeding 5%. These readings confirm the surge of total gas in the 950 - 1300 MSS interval. As evidenced by well M34, this accumulation poses a potential hazard during drilling operations. The gas typically resides within isolated sand bodies due to effective sealing mechanisms on the platform. Therefore, the document strongly advises exercising caution when drilling through this zone, recommending a reduction in the rate of penetration and an increase in mud weight to mitigate the risk of losses and potential blowouts. Continuous monitoring of total gas is critical to detect any sudden increases that may signal an imminent gas influx. The document also mentions anomalies at a depth interval between 1,000-1,300 when compared with the MSS its log cross section, was included in the marker interval Fs and Fs-s3-s2 (Figure 7).

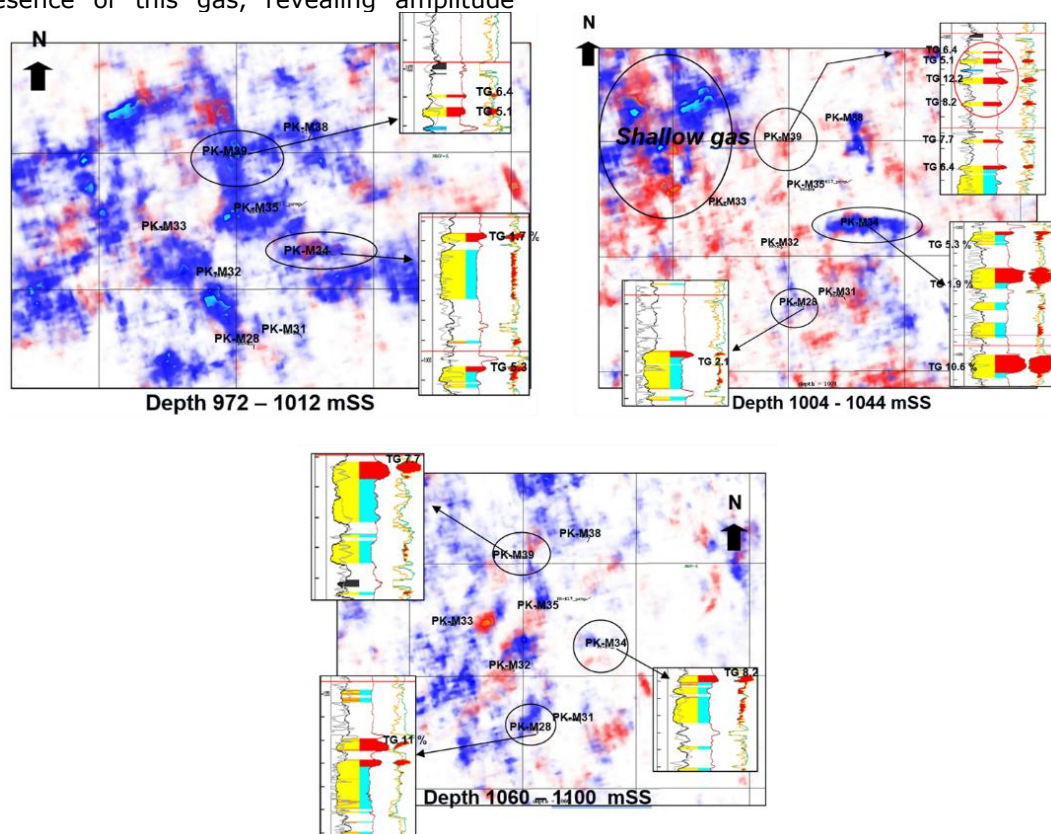


Figure 7. Map of gas bearing distribution along the Platform M, the gas indicated with black circle and shown in the log data.

CONCLUSION

In stratigraphic terms, the lithology within the study area—extending to a depth of approximately 1500 meters subsea (MSS)—defines what is referred to as the Shallow Zone. Based on core descriptions and master log cross-checks, this interval consists of alternating sandstone and mudstone layers.

In the eastern and southern parts of Platform M, deposition is dominated by distal delta front environments, where mouth bars become increasingly smaller and more isolated.

Shallow gas accumulations are concentrated between markers Fs-s2 and Fs-s3, corresponding to a depth range of 950–1300

MSS. These accumulations are often isolated and discontinuous, as confirmed by both well data and seismic interpretation. Gas in this interval is primarily composed of methane (C1), with only minor traces of heavier hydrocarbons (C2–C5), and occasionally exhibits gas-water contact features. Notably, significant surges of total gas are observed within this depth range, especially in wells such as M38.

Seismic amplitude anomalies in the 950–1300 MSS interval further support the presence of shallow gas pockets, although their visibility varies between wells—ranging from clear accumulations to faint, localized anomalies. This inconsistency in lateral distribution highlights the heterogeneity of the gas-bearing sandbodies and the potential drilling hazards they pose. The Gas-Bearing Reservoir Map confirms that these accumulations are indeed localized within isolated sandbodies, rather than being laterally extensive. Such confinement, combined with effective sealing in Platform M, increases the risk of pressure buildup and blowouts if not properly managed.

Therefore, in light of these findings, the 950–1300 MSS interval should not be simply evaded, but rather thoroughly characterized and incorporated into drilling planning. Mitigation strategies—such as adjusting casing points, pre-drill gas hazard modeling, and real-time gas detection—should be implemented to ensure safe and informed operations in the shallow zone. This approach allows operators to anticipate shallow gas zones proactively and reduces the likelihood of unexpected formation pressures during drilling.

REFERENCES

- Abraham, C. U., Clement, E. B., Anietie, E. E., & Monday, U. U. (2020). Sequence stratigraphic study of X field in eastern offshore of Niger Delta, Nigeria. *Journal of Geology and Mining Research*, 12(2), 65. <https://doi.org/10.5897/jgmr2019.0322>
- Al-Aziz, S. A., Al-Rowyeh, A., AL-Enezi, T., Chetri, H., & Al-Anzi, E. (2009). Sabiriyah Upper Burgan Geological Model and Reservoir Characterization. SPE Middle East Oil and Gas Show and Conference. <https://doi.org/10.2118/120380-ms>
- Allen, G.P dan Chambers, J.L.C., 1998. *Sedimentation in the modern and Miocene Mahakam Delta*. Indonesian Petroleum Association, 236p.
- Allen, G.P and F. Mercier. 1988. *Subsurface Sedimentology of Deltaic Systems*. Total Exploration Laboratory, Pessac, France: Pesa Journal, No.12, p.30-44
- Allen, G.P., Laurier, D., dan Thouvenin, J.M., 1979. *Etude sedimentologique du delta de la Mahakam*. TOTAL Compagnie Francaise des Petroles Notes Mem., **15**, 156p.
- Amalia, D. (2019). APPLICATION OF DIGITAL IMAGE TECHNOLOGY FOR DETERMINING GEOMETRY, STRATIGRAPHY, AND POSITION OF CRACKS INSIDE EARTH SLOPE. *International Journal of Geomate*, 17(63). <https://doi.org/10.21660/2019.63.25640>
- Asquith, G.B., 1982. *Basic Well Log Analysis for Geologists*. The American Association of Petroleum Geologists: Tulsa, Oklahoma USA
- Bachtiar, A. (2018, March 5). The Tertiary Paleogeography Of The Kutai Basin And Its Unexplored Hydrocarbon Plays. Proc. Indon Petrol. Assoc., 36th Ann. Conv. <https://doi.org/10.29118/ipa.0.13.g.126>
- Banerjee, A., & Salim, A. M. A. (2020). Seismic attribute analysis of deep-water Dangerous Grounds in the South China Sea, NW Sabah Platform region, Malaysia. *Journal of Natural Gas Science and Engineering*, 83, 103534. <https://doi.org/10.1016/j.jngse.2020.103534>
- Chen, Z. (2018). Research on Constrained Sedimentary Facies Reservoir by Well-seismic Inversion. *IOP Conference Series Earth and Environmental Science*, 189(4), 42024. <https://doi.org/10.1088/1755-1315/189/4/042024>
- Colke, I. R., Craig, J., & Blundell, D. J. (1999). Structural controls on the hydrocarbon and mineral deposits within the Kutai Basin, East Kalimantan. *Geological Society London Special Publications*, 155(1), 213. <https://doi.org/10.1144/gsl.sp.1999.155.01.16>
- Combaz, A. dan de Matharel, M., 1978, *Organic Sedimentation and Genesis of Petroleum in the Mahakam Delta, Borneo*, American Association of Petroleum Geologists Bull. V. 62, p. 1684 – 1695
- Drake, W. R., Hawkins, S. J., & Lapierre, S. G. (2013). The Role of Stratigraphic Architecture in Resource Distribution: An Example from the Niobrara Formation of the Denver-Julesburg Basin. Unconventional Resources Technology Conference, Denver, Colorado, 12-14 August 2013, 2465. <https://doi.org/10.1190/urtec2013-257>
- Gastaldo, R.A dan Huc, A.Y., 1992. *Sediment facies, depositional environments, and distribution of Phytoclasts in the recent Mahakam River Delta, Kalimantan, Indonesia*. *Palaos* **7**, 574-590.
- Graña, D., Paparozzi, E., Mancini, S., & Tarchiani, C. (2012). Seismic driven probabilistic classification of reservoir facies for static reservoir modelling: a case history in the Barents Sea. *Geophysical*

- Prospecting, 61(3), 613.
<https://doi.org/10.1111/j.1365-2478.2012.01115.x>
- Hasan, R. A., Saberi, M. H., Riahi, M. A., & Manshad, A. K. (2023). Electro-facies classification based on core and well-log data. *Journal of Petroleum Exploration and Production Technology*, 13(11), 2197. <https://doi.org/10.1007/s13202-023-01668-5>
- Keynejad, S., Sbar, M. L., & Johnson, R. A. (2020). Creating probabilistic 3D models of lithofluid facies using machine-learning algorithms. *Interpretation*, 8(4). <https://doi.org/10.1190/int-2019-0249.1>
- Kompanik, G. S., HEIL, R., Al-Shammari, Z. A., & Al-Shammery, M. J. (1993). *Geologic Modelling for Reservoir Simulation: Hanifa Reservoir, Berri Field, Saudi Arabia*. Middle East Oil Show. <https://doi.org/10.2118/25580-ms>
- Koning, T., Cameron, N., & Clure, J. (2021). Undiscovered Potential in the Basement Exploring in Sumatra for oil and gas in naturally fractured and weathered basement reservoirs. *Berita Sedimentologi*, 47(2), 67. <https://doi.org/10.51835/bsed.2021.47.2.320>
- Mora, Stefano et. Al, 2000. *Modern, Ancient Deltaic Deposits and Petroleum system of Mahakam Area*. IPA 2002 Field Trip Guide Book, TOTALFINAELF E&P INDNESIE, Balikpapan
- Nainggolan, T. B., Nurhasanah, U., & Setiadi, I. (2021). Depositional sequence interpretation using seismic and well data of offshore Central Sumatra Basin. *IOP Conference Series Earth and Environmental Science*, 944(1), 12002. <https://doi.org/10.1088/1755-1315/944/1/012002>
- Napitupulu, V., Jannah, M., Silaen, M., & Darman, H. (2021). Hydrocarbon Columns of Oil and Gas Fields in the South Sumatra Basin. *Berita Sedimentologi*, 46(1), 51. <https://doi.org/10.51835/bsed.2020.46.1.60>
- Nur, A., Hatta, M. P., Thaha, M. A., & Suriamihardja, D. A. (2020). Preliminary sediment modeling at the confluence of the Mahakam and Karang Mumus River. *IOP Conference Series Earth and Environmental Science*, 419(1), 12129. <https://doi.org/10.1088/1755-1315/419/1/012129>
- Pendkar, N., Zainun, F., Parsuram, S. N., Aziz, A., Ali, M. F., & Embi, R. Bt. (2014). Sedimentology and Diagenesis of Deeper Clastic Reservoirs: Some Insights from Recent Exploration Wells in Offshore Sarawak, Malaysia. *All Days*. <https://doi.org/10.2523/iptc-18038-ms>
- Syed, M. S., Khan, F. A., Farid, A., Khan, A., & Hasnain, N. S. and K. (2008). Presenting seismic stratigraphy and attribute analysis as pioneer techniques for delineation of reservoir quality sand bodies in Indus offshore, southwest Pakistan. *GEO 2008*. <https://doi.org/10.3997/2214-4609-pdb.246.340>
- Yang, H., Fan, T., & Zhou, M. (2023). Study on tight reservoir law and prediction of favorable areas - Take Wangjiawan well block Wang 107 as an example. *E3S Web of Conferences*, 385, 3031. <https://doi.org/10.1051/e3sconf/202338503031>

